Korean J. Chem. Eng., **21**(1), 296-302 (2004)

Imaging Nanostructured Fluids Using Cryo-TEM

You-Yeon Won†

School of Chemical Engineering, Purdue University, West Lafayette, IN 47907, USA
(*Received 16 October 2003 • accepted 29 October 2003*)

Abstract−Cryogenic transmission electron microscopy (cryo-TEM) has gained increasing popularity among researchers in the field of amphiphilic self-assembly as an experimental method of choice because of its unique ability to visualize nanostructures in complex fluids. Due to many recent technical improvements in the instrumentation, cryo-TEM experiments are now common. However, some limitations and possible artifacts are still a problem, and awareness of them remains a prerequisite for reliable operations and interpretation. The goal of this paper is to provide a review of the basic methods and procedures by which the cryo-TEM experiments are typically practiced. As examples, this paper also presents recent results derived from our cryo-TEM studies of micellization of block copolymer blends which clearly illustrate the unique usefulness of the technique for exploring the unexpected, complex, and/or heterogeneous nanostructures in amphiphilic solutions.

Key words: Cryo-TEM, Micelle, Self-assembly, Block Copolymer, Blend

INTRODUCTORY REMARKS

Considering that light microscopes have limited image resolution that is imposed by the wavelength of visible light, transmission electron microscopy (TEM) is the only technique that provides nanometer-scale resolution real-space images of three-dimensional objects. The application of TEM to direct visualization of colloidal fluid nanostructures requires rapid vitrification of the samples, and so the technique is referred to as cryogenic TEM or cryo-TEM. Due to its unique ability to visualize the actual nanostructures in complex fluids at high water content, cryo-TEM has gained increasing popularity among researchers who study the amphiphilic self-assembly. Clearly, this has been reflected in the dramatically increased number of cryo-TEM-based research publications over the last decade.

In the mid 80s a group of structural biologists first demonstrated a practical method of vitrifying aqueous samples in the form of thin films and the feasibility of TEM imaging of such samples [Adrian et al., 1984]. Soon after this initial breakthrough that came amidst studies of biological specimens such as viruses, the specific procedure for rapid freezing was quickly adopted in visualization of surfactant solutions. In the late 80s and early 90s, participation of chemical engineers in experimental developments of cryo-TEM resulted in many significant advances that contributed to the creation of the structural pictures of various surfactant micelles that we accept today. Examples of these later advances include the introduction of a temperature- and humidity-controlled chamber for equilibration of the specimen prior to plunge vitrification (often referred to as the controlled environment vitrification system or CEVS) [Bellare et al., 1988], the rationalization of the freezing process and the identification of the best practical cryogens through heat transfer and thermodynamic analyses [Bailey and Zasadzinski, 1991; Zasadzinski, 1988], and the establishment of a fundamental understanding of the contrast mechanisms for cryo-TEM [Bellare, 1988; Chiruvolu et al., 1996].

Cryo-TEM, which can visualize objects as small as 1 nm [Bellare, 1988], is uniquely suited for identifying the local nanostructures in amphiphilic solutions. Examples of novel morphologies discovered in conventional surfactants by cryo-TEM are numerous. Branched wormlike micelles first proposed to explain anomalous rheological behaviors of cetylpyridinium chloride (CPCl) wormlike micelles in hexanol/water with excessive sodium chloride (NaCl) [Porte et al., 1986] have been microscopically confirmed in both mixed [Harwigsson et al., 1994; Lin, 1996; Silvander et al., 1996] and single-amphiphile [Danino et al., 1995; Jain and Bates, 2003; Won et al., 2002] systems. Among the most fascinating findings with cryo-TEM are exquisite intermediate-like structures such as perforated vesicles (i.e., vesicles with regular holes) that have been documented with mixed amphiphilic systems such as lecithin/cetyltrimethylammonium chloride (CTAC)/brine [Edwards et al., 1993] and lecithin/sodium dodecyl sulfate (SDS)/brine [Silvander et al., 1996]. It is not only micelles or vesicles but also various ordered liquid-crystalline structures that have been successfully identified by means of cryo-TEM; examples include dispersed particles of the cubic Q^{229} phase (dubbed "cubosomes") in a solution of Pluronic, i.e., poly(ethylene oxide-*b*-propylene oxide-*b*-ethylene oxide) [Almgren et al., 1996], and bundles of inverted hexagonal cylinders (so-called "hexosomes") in a ternary dioleylphosphatidylethanolamine/CTAB/water mixture [Gustafsson et al., 1995]. The structures of DNA molecules and their complexes with other substances such as proteins are also well-documented subjects of cryo-TEM [Dubochet et al., 1992]. For instance, cryo-TEM investigation of DNA ejected from bacterial viruses into aqueous solution containing polyvalent counterions resulted in a new discovery of the mechanisms by which the toroidal DNA condensates of controlled size can be fabricated [Lambert et al., 2000].

With the advances in synthetic techniques, new amphiphilic ma-

†To whom correspondence should be addressed.
E-mail: yywon@ecn.purdue.edu
‡This paper is dedicated to Professor Hyun-Ku Rhee on the occasion of his retirement from Seoul National University.

terials are continually created, and cryo-TEM has become an essential tool for exploring their self-assembling behaviors. For instance, application of cryo-TEM to characterization of the poly(ethylene oxide-*b*-butadiene) surfactants led to observations of intriguing stable network structures that qualitatively differentiate the self-assembling behavior of the polymeric surfactants from their small molecule equivalents [Jain and Bates, 2003]. Cryo-TEM is also capable of making available structural information of gel-like solutions, as has been demonstrated with the unforeseen foamy structures of block copolypeptide amphiphilies [Pochan et al., 2002]. Future new applications of the cryo-TEM technique are much more likely to be related to the development of new amphiphilic materials that have properties tailored for specific ultimate applications.

Recent years have seen significant technical improvements on the instrumentation side; the CEVS equipment became commercially available (e.g., Cryoplunge from Gatan, Inc. http://www.gatan.com/), and the conducting of cryo-TEM operations became handy after digital imaging was incorporated into the common practice [Danino et al., 2001]. Also, modification of the CEVS device design is continually sought [Egelhaaf et al., 2000; Kasas et al., 2003]. All these factors have in fact resulted in increased utilization of cryo-TEM by non-experts. Although cryo-TEM is widely accepted as a reliable technique of choice for direct visualization of nanostructured fluids, there exist limitations and possible problems of instrumentation, and awareness of the possible artifacts and understanding of their mechanisms are prerequisites for reliable operations of the experiments and interpretation of the results. An important aim of the present paper is to review the basic methods and procedures by which the cryo-TEM experiments are typically practiced. This survey therefore reflects the current state of the cryo-TEM techniques. Previous reviews should also be referred to if one wants to learn to a greater extent specific topics such as contrast mechanisms [Bellare, 1988; Chiruvolu et al., 1996], common artifacts [Talmon, 1987, 1996], and limitations on the types of phase structures that can be studied [Almgren et al., 1996]. In the present paper, the review section will be followed by sample results from our mixed block copolymer micellization studies which we present as an illustration of the unique usefulness of cryo-TEM.

DISCUSSION OF THE METHODS

1. Sample Preparation

TEM imaging of nanostructures of the water-borne aggregates can be obtained only through rapid vitrification of the liquid samples in the form of thin films. The frozen hydrated specimens are normally compatible with the high vacuum operation of the TEM instrument (typically, ~10^{-5} Pa [Williams and Carter, 1996]), and are free of molecular thermal motions that would otherwise blur the image. Such cryogenic fixation of the fluid sample is much preferable to the conventional staining-and-drying approaches because of the labile character of the self-assembled structures in amphiphilic solutions [Talmon, 1983]; this is particularly true when one has to deal with small molecule amphiphiles. It has only been twenty years since thermal fixation of a water-based specimen and direct imaging of the frozen sample based on natural contrasts were first proved to be feasible [Adrian et al., 1984]. The key step in that initial development in cryo-TEM sample preparation was the high-speed cooling that involves mechanical plunging of the specimen into a reservoir of cryogen, typically liquid ethane (or less preferably propane) cooled by liquid nitrogen. Currently, most researchers adopt the essentially same combination of choices for the cooling method and material which enables one to achieve a cooling rate of more than 10^4 K/s which is needed to vitrify the water-based systems [Mayer, 1985]. The vitrification is normally performed at temperatures close to the freezing point of the cryogen [Costello and Corless, 1978; Gulik-Krzywicki and Costello, 1978; Mayer, 1985], and the choice of ethane is mainly because it offers a minimal amount of cryogen boiling upon contact with the specimen which enhances the heat transfer between the sample and the cryogen [Bennett and Myers, 1982], through the combined mechanisms of cryogen convection and evaporation [Bailey and Zasadzinski, 1991; Zasadzinski, 1988].

The sample thickness threshold for the avoidance of the multiple scattering that leads to image deterioration and for optimal phase contrast imaging is approximately 200 to 400 nm for the range of incident electron energy between 100-200 kV; this thickness upper limit simply reflects the mean free path for elastic scattering of the electron at the corresponding energy [Williams and Carter, 1996]. Specimen films of this thickness or less can be achieved by using a holey polymer film supported on a standard TEM metal grid, typically made of copper. The holey film is usually made from hydrophobic polymers such as cellulose acetate butyrate [Vinson, 1988] or poly(vinyl formal) (Ted Pella, Inc. http://www.tedpella.com/), and coated with carbon for enhancement of the mechanical stability under electron radiation. Polymer films with holes of between 1 and 10 μm can be fabricated through the sequence of condensation of ice crystals on a chilled substrate, dip coating of the polymer solution, and evaporation of water and the organic solvent [Vinson, 1988].

In order that the thin samples are vitrified at a chosen equilibrium condition, the preparation environments have to be carefully controlled throughout the procedures for the thin film formation. For this reason, the sample preparation is usually performed in an isolated chamber, often referred to as the controlled environmental vitrification system (CEVS) originally designed by the Minnesota school of cryo-TEM [Bellare et al., 1988]. Avoidance of any water evaporation from the sample is achieved by humidification of the chamber to near saturation of water, and the temperature is typically controlled by air circulation to within 0.1 °C. In the CEVS, the fluid sample in the form of a ~5 μL droplet is placed on the microperforated cryo-TEM grid. It is then blotted by a filter paper, resulting in the formation of thin liquid films of normally 10 to 250 nm thickness, freely spanning across the micropores in a carbon vapor-deposited holey polymer layer supported by a metal TEM grid. After a period of equilibration (e.g., approximately 30 seconds for small molecule surfactants at room temperature), the sample grid assembly is plunged into a reservoir of liquid ethane at its melting temperature (~90 K) at a speed of about 2 to 4 m/s. The delay is necessary for relaxation of the possible flow-induced deformation caused by the blotting process, if one intends to investigate the equilibrium nanostructures [Clausen et al., 1992; Li et al., 1995]. Time-resolved studies of dynamic events are also possible by application of on-the-grid processing, e.g., pH-jump [Siegel et al., 1989], temperature-jump [Karlstrom et al., 1990], spray mixing [Unwin, 1995], or flow-induced deformation [Zheng et al., 2000]. Along

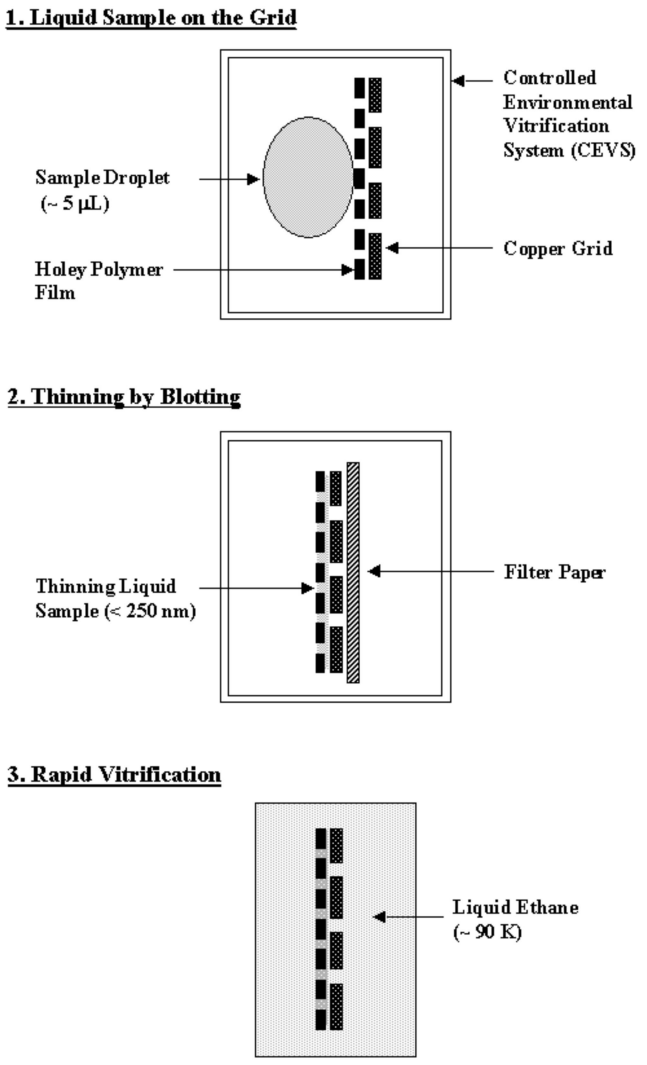

Fig. 1. Schematic illustration of the sample preparation procedures for cryo-TEM.

these lines, one notable recent advance is the introduction of the so-called vitrification robot (Vitrobot, Maastricht Instruments http://www.maastrichtinstruments.com/projects/vr/), a computer-controlled plunger with an environmental chamber which enables time-resolved sampling with a millisecond temporal resolution upon automated triggering of the desired dynamic processes. The procedures for the cryo-TEM sample preparation in the CEVS are summarized in Fig. 1. Subsequent TEM examination of the vitrified specimen is performed at liquid nitrogen temperature (~−180 °C) using a commercial cryostage (e.g., Gatan 626 from Gatan, Inc. http://www.gatan.com/).

2. Phase Contrast

The cryogenic fixation renders the sample inherently incompatible with the implementation of the heavy-metal staining approaches for artificial enhancement of the mass-thickness (amplitude) contrast. However, despite the tiny difference in electron density between the hydrocarbon substances and the frozen aqueous background, direct imaging of the microstructures of the surfactant aggregates has proven possible through the mechanism known as phase contrast [Adrian et al., 1984]. Phase contrast arises from the constructive interference between the scattered and unscattered electromagnetic waves in the elastic scattering of electrons, and can be achieved by the effect of defocus. Defocus of the objective lens (Δf) induces a phase shift (χ) of the scattered electrons in reciprocal space:

$$\chi \approx \pi \Delta f \lambda q^2 + \frac{1}{2}\pi C_s \lambda^3 q^4 \quad (1)$$

where λ is the electron wavelength, q is the magnitude of the momentum transfer vector, and C_s is the spherical aberration of the objective lens [Bellare, 1988; Chiruvolu et al., 1996; Williams and Carter, 1996]. Since the intensity of the image has a squared-sinusoidal dependence on the phase shift, i.e., $I \sim \sin^2\chi$, the optimal defocus Δf corresponds to the first maximum of $\sin^2\chi$ (that is, $\chi = \pm\pi/2$), and depends on the size of the object probed (~1/q).

3. Possible Artifacts

Perhaps the sole artifact that cannot be avoided is the size segregation of the dispersed particles. The freely suspended liquid films are typically wedge-shaped, and the thickness variations in the specimen films result in the non-uniform distribution of the colloidal particles. Large particles of size greater than the thickness of the film at the center are size-excluded from the central area and concentrated around the edge of the hole where the film thickness is greater. We also note that only the structures in a size range less than several hundreds nanometers can comfortably fit within the sample film. In this sense, cryo-TEM, though convincing as a local-microstructural probe, does not provide reliable information on the length scale greater than the confining thickness.

The blotting process may have a significant effect on the structures observed in the frozen specimens. The deformation rate during the blotting may reach 10^5 reciprocal seconds [Talmon, 1996], thereby possibly resulting in structural rearrangements of the aggregates or even possibly phase transitions. Such effects have been evidenced as flow-induced alignments of the cylindrical micelles [Clausen et al., 1992; Li et al., 1995] and as flow-induced structural transitions of the micelles and vesicles [Zheng et al., 2000]. The shear effects are a controllable artifact in the sense that the CEVS permits an unperturbed detainment for restoration of the deformed sample, and are sometimes intentionally used for studying the mechanisms of the aforementioned dynamic processes by successive sampling of the transient stages in progress on grid.

Upon vitrification, the cryo-TEM specimens become susceptible to surface contamination which may lead to misinterpretation of the image. Common sources from which contaminants condense on the cold specimen are TEM vacuum leaks and wet photographic films, and therefore clean vacuum conditions during instrumentation are key to reduction of contamination. In the absence of the astigmatism, the crystalline deposition usually appears darker than the vitreous ice or the frozen amorphous hydrocarbons due to the different inner electron potentials. Also, when the TEM is operated slightly out of focus, the surface contaminants are distinguished from the objects confined within the film by broader Fresnel fringes due to the difference in vertical position.

Exposure of the sample to the electron beam may introduce irreversible damages on the frozen specimen which include the ice conversion of the vitreous water and various types of local radiolysis [Talmon, 1987, 1996]. All these effects are caused by the energy deposition that results from the inelastic interaction of electrons with

the sample. It is, therefore, desirable to minimize the electron exposure prior to and even during the imaging ($<10^2$ $e^-/Å^2$) [Talmon, 1987] through the use of the minimal dose system (MDS) with which all the modern TEM instruments are equipped.

4. TEM Equipment and Imaging Procedures

All cryo-TEM images presented in this paper, for example, were obtained by using a JEOL 1210 operating at 120 kV. The use of a minimal dose system (MDS) was necessitated by the electron radiation sensitivity of the frozen hydrated samples probed in this research. Adequate phase contrast was achieved at a nominal underfocus of between 3 and 26 μm. Images were recorded on a Gatan 724 multiscan digital charge-couple device (CCD) camera, and subsequently processed with analysis software of DigitalMicrographs version 3.1 or higher. It is worth noting that the CCD camera based-digital imaging has multiple advantages over the conventional methods using negative films: reduced sample contamination, imaging at a lower electron dose, higher accessible magnification, and real-time data acquisition [Danino et al., 2001]. These aspects are clearly illustrated in the dramatically improved quality of the images that have been documented in recent years [Won et al., 1999, 2002; Zheng et al., 1999]. The optical density gradient of the background which is normally ramp-shaped often leads to contrast and brightness deficiencies. This can be digitally corrected by using a background reconstructed by obtaining a least square fit of a surface function which approximates the original background without the specimen images. A subroutine for the background subtraction that is compatibilized with the DigitalMicrographs software is available. All the pictures presented in Section 3 are typical examples of the background-subtracted digital images.

CRYO-TEM OF MICELLES OF BLOCK COPOLYMER BLENDS: RECENT EXAMPLES

In terms of the relevant length scales at which the structural properties in amphiphilic solutions are probed (i.e., approximately from 1 nm to 100 μm), cryo-TEM is quite comparable to scattering techniques. The direct outcome of scattering experiments is, however, reciprocal space information, and therefore, inference of the real-space structure normally requires combined procedures of assumption of a structural model and its comparison with the experimental results. Cryo-TEM, on the other hand, directly provides the structural information. In this sense, application of cryo-TEM becomes very necessary when one explores the self-assembly behaviors of such materials in which the resultant structures are not easy to predict or are expected to be morphologically complex and heterogeneous. In what follows, we describe recent results from our cryo-TEM studies of micellization of block copolymer blends (i.e., mixtures) which clearly illustrate that the technique is uniquely suited for the exploratory nanostructural investigation of amphiphilic solutions.

1. Materials

Two poly(ethylene oxide-*b*-1,2-butadiene) (PEO-PB) diblock copolymers were used for this study. The synthesis and characterization of these copolymers have been described in our previous publication [Hillmyer and Bates, 1996; Won, 2000]. The molecular characteristics and also the resulting morphologies formed in water identified by cryo-TEM [Won et al., 2002] are summarized in Table 1. Solutions containing 1 wt% OB1/OB2 mixtures were prepared in two different ways: mixing of the two polymers before (*premixing*) or after (*postmixing*) hydration. In the former case, the weighed mixtures of the two block copolymers were first homogeneously dispersed in chloroform, dried, annealed in a vacuum oven at 50 to 60 °C for several hours, and then dissolved with an appropriate amount of water (HPLC grade, Aldrich) at room temperature. The *postmixed* sample was prepared simply by mixing a premade 1% OB1 solution with a premade 1% OB2 solution. Then the sample was sealed and stirred at room temperature with a magnetic stirring bar rotating at several Hz until complete dissolution. All the solution samples were equilibrated for at least five days, and the morphological characterization was carried out after the polymers were completely dispersed without any macroscopic heterogeneity in the sample as judged by the naked eye. The composition data for binary mixtures of OB1 and OB2 are listed in Table 2.

Table 1. Molecular characteristics of pure block copolymers

Sample ID	Chemical identity	$M_{n,\,total}$	$M_{n,\,PB}$	f_{EO}	PDI	Structures[a]
OB1	PEO-PB	8.1	2.5	0.66	1.13	S
OB2	PEO-PB	3.6	2.5	0.28	1.13	B

[a]Aggregation morphologies formed in water identified with cryo-TEM: B=bilayered vesicle; S=sphere. M_n is the number-average molecular weight in units of kg/mol, and f_{EO} is the melt volume fraction of PEO calculated from the reaction stoichiometry using the amorphous densities estimated from published data for PB and PEO at room temperature (i.e., $d_{90\%1,\,2\text{-}PB}\approx 0.87$ g/cm^3, and $d_{PEO}\approx 1.13$ g/cm^3) [Fetters et al., 1994].

Table 2. Mixtures from OB1 and OB2

$<f_{EO}>$	Molar ratio (OB1 : OB2)	Preparation	Structures[a]
0.45	0.38 : 1	Premixed	B, C
0.54	1 : 1	Premixed	C
0.59	2 : 1	Premixed	C, S
0.64	10 : 1	Postmixed	S, B, C

[a]Coexisting structures are listed in the order of abundance: B=bilayered vesicle; C=cylinder; S=sphere. $<f_{EO}>$ is the overall PEO volume fraction in the mixture.

2. Results and Discussion

Use of binary mixtures of block copolymers may be an efficient route to producing intermediate structures. The aggregation behaviors of the *premixed* block copolymers of OB1 (spherical micelles, f_{EO}=0.66) and OB2 (vesicles, f_{EO}=0.28) at intermediate overall PEO compositions of $<f_{EO}>$=0.45, 0.54, and 0.59 were examined by cryo-TEM.

At $<f_{EO}>$=0.45, the 1% solution of the OB1/OB2 (0.38 : 1 by mole) mixture exhibits not only cylindrical micelles anticipated at this overall PEO content but also a spectrum of aggregates including vesicles, various hybrid structures, and rare remnants of spherical micelles, as shown in Figs. 2A to 2C. At an identical PEO composition (f_{EO}=0.45), the pure diblock PEO-PB forms neat cylinders when dissolved in excess water (Figs. 2A and 2B in ref. [Won et al., 2002]). The disparity illustrates some limitation in predicting

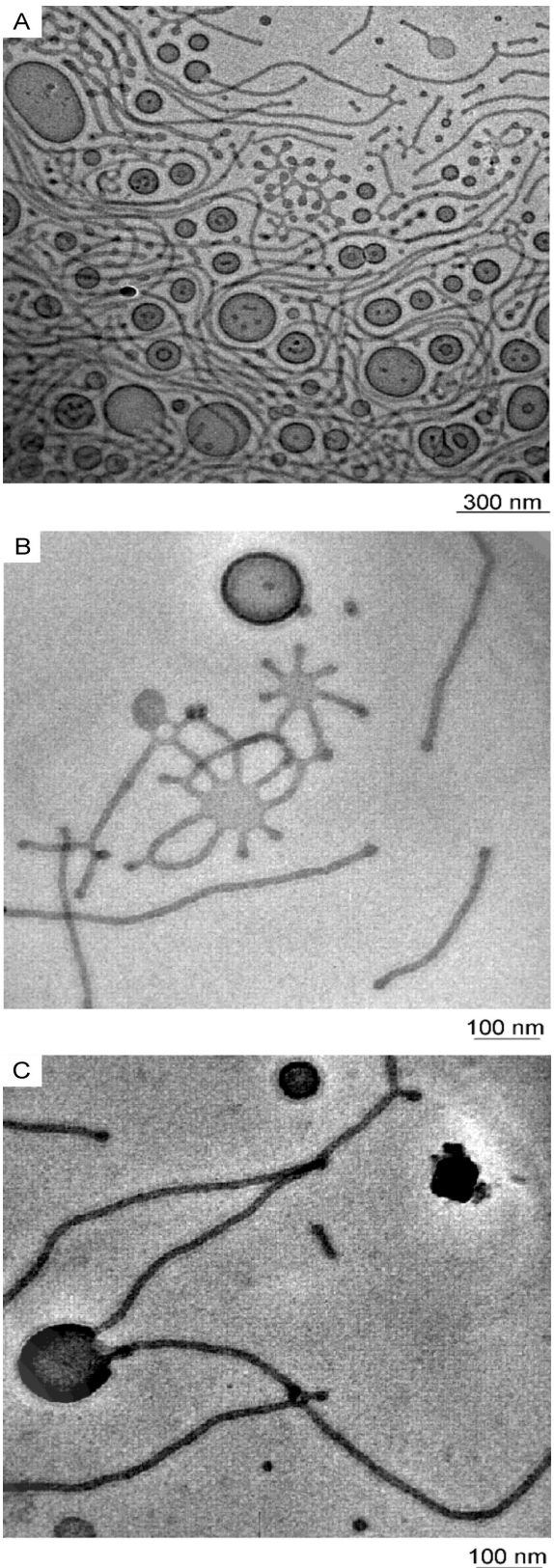

Fig. 2. Cryo-TEM micrograph of a 1.0 wt% premixed OB1/OB2 (0.38 : 1 by mole) in water with $<f_{EO}>$=0.45. Images taken at 16 days (A) and 13 months (B and C) after the sample preparation display common qualitative features in structure, indicating that the observed behavior at this OB1/OB2 ration is not transient.

the behaviors of mixed systems. The observed compound structures such as alveoli, thicker cylinders, membrane flakes, and unraveling vesicles rather closely mimic those previously reported for a PEO-based triblock with a comparable PEO volume fraction f_{EO}= 0.44 but with a higher polydispersity index (Figs. 7A to 7D in ref. [Won et al., 2002]).

The image taken for a 1% solution containing an equimolar mixture of OB1 and OB2 ($<f_{EO}>$=0.54) displays predominant cylindrical micelles with some localized small protuberances (Fig. 3). The diminished concentration of defects and heterogeneous structures indicates that the intermediate curvature may be best produced at the stoichiometric molar ratio between two block copolymers having the same hydrophobic PB volume per chain but differing in the

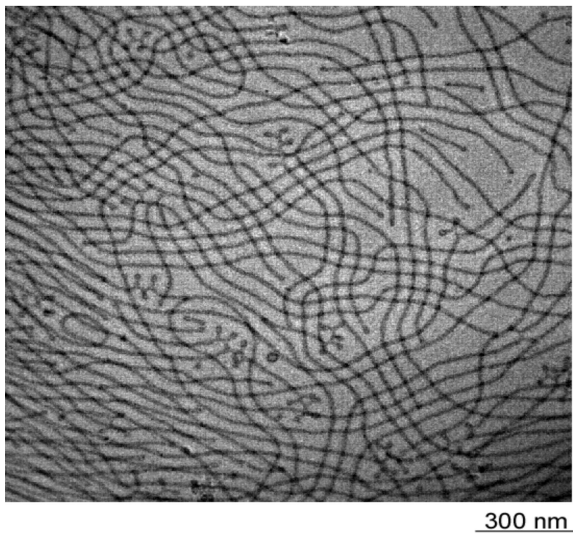

Fig. 3. Cryo-TEM micrograph of a 1.0 wt% premixed OB1/OB2 (1 : 1 by mole) in water with $<f_{EO}>$=0.54. The premixing was done 6 days before the cryo-TEM experiments.

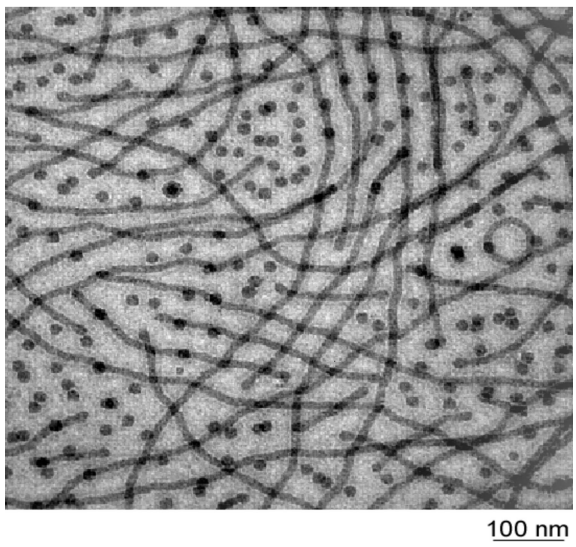

Fig. 4. Cryo-TEM micrograph of a 1.0 wt% premixed OB1/OB2 (2 : 1 by mole) in water with $<f_{EO}>$=0.59. The premixing was done 9 months before the cryo-TEM experiments.

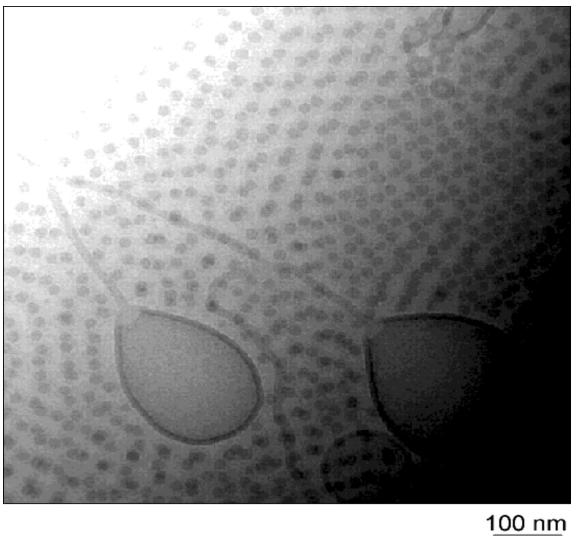

Fig. 5. Cryo-TEM micrograph of a 1.0 wt% postmixed OB1/OB2 (10 : 1 by mole) in water with $<f_{EO}>$=0.64. The postmixing was done 9 months before the cryo-TEM experiments.

hydrated PEO volume per chain.

A 2 : 1 OB1/OB2 mixture (f_{EO}=0.59) forms higher-curvature structures such as short cylinders coexistent with spheroidal micelles (Fig. 4). A wealth of globular micelles indicates that OB1 is in excess of OB2 in creating the intermediate structure (i.e., cylinders).

The mixed block copolymer solutions exhibit a pronounced dependence on sample history. This was illustrated in observations of a *postmixed* OB1/OB2 (10 : 1) solution with $<f_{EO}>$=0.64. The cryo-TEM imaging was performed nine months after the sample preparation. The existence of transient structures such as unraveling vesicles displayed in a representative image (Fig. 5) represents evidence for extremely slow structural redistribution between the two types of aggregates, which is also consistent with our separate experiments on molecular exchange in PEO-PB micelles using small-angle neutron scattering (SANS) [Won et al., 2003]. The preserved coexistence between spheres and vesicles after nine months of storage is in clear contrast to the complete extermination of vesicles exhibited even at lower overall PEO compositions by the *premixed* OB1/OB2 solutions (Fig. 3 and Fig. 4).

Experiments performed with the mixed OB1/OB2 block copolymers of the same PB size but different f_{EO} identifies that the aggregation behavior of a mixture with an overall PEO volume fraction $<f_{EO}>$ is not identical to that of a pure diblock copolymer with f_{EO}= $<f_{EO}>$; compare Fig. 2 in ref. [Won et al., 2002] and Fig. 2 in the present paper for example. Near an OB1/OB2 molar ratio of unity, a fairly homogeneous intermediate structure was formed (Fig. 3), while at asymmetric ratios, the structure that appears to be formed solely by the excess species was found to coexist with the intermediate morphology (Figs. 2 and 4). The results indicate that there exists an optimal proportion at which the two amphiphilic copolymers are best delocalized to produce the intermediate structure, and therefore proper care should be taken in utilizing the blending approach for tuning the micelle morphology.

Use of block copolymer mixtures provides an alternative route for creating a desired microdomain shape. As evidenced in the images taken from the mixtures of two different PEO-PBs, the neat structure that possesses a preferred intermediate curvature was obtained only at a specific mixing ratio at which delocalization of the two components is maximized. At the other ratios, different structures mutually coexisted, and the distribution of the coexisting aggregation structures correlated with the overall PEO composition. The path taken for sample preparation played a crucial role in determining the micelle morphology, and to obtain a better mixing two polymers had to be mixed before being dissolved with water. The results also indicate that molecular exchange in PEO-PB micelles is negligible, and the intermicellar equilibration time can be of the order of many years. Therefore, though stable over a long period of time, the recorded micelle structures are not the equilibrium ones.

CONCLUDING REMARK

This paper presents a brief review of the basic methods and procedures for cryo-TEM. Sample results from our studies of micellization of block copolymer blends that illustrate the unique usefulness of the technique are also described. The past 20 years of development reflected in the current state of the techniques has established cryo-TEM as one of the most powerful nanostructural characterization tools available to researchers in the field of amphiphilic self-assembly. The future of cryo-TEM application should hold many exciting new discoveries, which await further improvements in the cryo-TEM instrumentation and developments of new amphiphilic materials tailored for advanced nanotechnological applications.

ACKNOWLEDGMENTS

The author wishes to thank Professors F. S. Bates and H. T. Davis (University of Minnesota) for their guidance on the research work from which the sample results are derived.

REFERENCES

Adrian, M., Dubochet, J., Lepault, J. and McDowall, A. W., "Cryo-Electron Microscopy of Viruses," *Nature*, **308**, 32 (1984).

Almgren, M., Edwards, K. and Gustafsson, J., "Cryotransmission Electron Microscopy of Thin Vitrified Samples," *Current Opinion in Colloid and Interface Sci.*, **1**, 270 (1996).

Bailey, S. M. and Zasadzinski, J. A. N., "Validation of Convection-Limited Cooling of Samples for Freeze-Fracture Electron Microscopy," *J. Microsc.-Oxford*, **163**, 307 (1991).

Bellare, J. R., "Cryo-Electron and Optical Microscopy of Surfactant Microstructures," Ph.D. Thesis, University of Minnesota, Minneapolis (1988).

Bellare, J. R., Davis, H. T., Scriven, L. E. and Talmon, Y., "Controlled Environment Vitrification System: An Improved Sample Preparation Technique," *J. Electron Micr. Tech.*, **10**, 87 (1988).

Bennett, C. O. and Myers, J. E., "Momentum, Heat, and Mass Transfer," McGraw-Hill, New York (1982).

Chiruvolu, S., Naranjo, E. and Zasadzinski, J. A., "Microstructure of Complex Fluids by Electron Microscopy," Structure and Flow in Surfactant Solutions, Herb, C. A. and Prud'homme, R. K., eds., Am. Chem. Soc., Washington, DC, 86 (1996).

Clausen, T. M., Vinson, P. K., Minter, J. R., Davis, H. T. and Talmon,

Y., "Viscoelastic Micellar Solutions: Microscopy and Rheology," *J. Phys. Chem.*, **96**, 474 (1992).

Costello, M. J. and Corless, J. M., "Direct Measurement of Temperature Changes within Freeze-Fracture Specimens during Rapid Quenching in Liquid Coolants," *J. Microsc.-Oxford*, **112**, 17 (1978).

Danino, D., Bernheim-Groswasser, A. and Talmon, Y., "Digital Cryogenic Transmission Electron Microscopy: An Advanced Tool for Direct Imaging of Complex Fluids," *Colloids and Surfaces A*, **183-185**, 113 (2001).

Danino, D., Talmon, Y., Levy, H., Beinert, G. and Zana, R., "Branched Thread-like Micelles in an Aqueous Solution of a Trimeric Surfactant," *Science*, **269**, 1420 (1995).

Dubochet, J., Adrian, M., Dustin, I., Furrer, P. and Stasiak, A., "Cryoelectron Microscopy of DNA Molecules in Solution," *Methods Enzymol.*, **211**, 507 (1992).

Edwards, K., Gustafsson, J., Almgren, M. and Karlsson, G., "Solubilization of Lecithin Vesicles by a Cationic Surfactant: Intermediate Structures in the Vesicle-Micelle Transition Observed by Cryo-Transmission Electron Microscopy," *J. Colloid Interface Sci.*, **161**, 299 (1993).

Egelhaaf, S. U., Schurtenberger, P. and Muller, M., "New Controlled Environment Vitrification System for Cryo-Transmission Electron Microscopy: Design and Application to Surfactant Solutions," *J. Microsc.-Oxford*, **200**, 128 (2000).

Fetters, L. J., Lohse, D. J., Richter, D., Witten, T. A. and Zirkel, A., "Connection between Polymer Molecular Weight, Density, Chain Dimensions, and Melt Viscoelastic Properties," *Macromolecules*, **27**, 4639 (1994).

Gulik-Krzywicki, T. and Costello, M. J., "Use of Low-Temperature X-ray Diffraction to Evaluate Freezing Methods Used in Freeze-Fracture Electron Microscopy," *J. Microsc.-Oxford*, **112**, 103 (1978).

Gustafsson, J., Arvidson, G., Karlsson, G. and Almgren, M., "Complexes between Cationic Liposomes and DNA Visualized by Cryo-TEM," *BBA-Biomembranes*, **1235**, 305 (1995).

Harwigsson, I., Soderman, O. and Regev, O., "Diffusion and Cryo-Transmission Electron Microscopy Studies of Bicontinuous Micellar Solutions," *Langmuir*, **10**, 4731 (1994).

Hillmyer, M. A. and Bates, F. S., "Synthesis and Characterization of Model Polyalkane-Poly(ethylene oxide) Block Copolymers," *Macromolecules*, **29**, 6994 (1996).

Jain, S. and Bates, F. S., "On the Origins of Morphological Complexity in Block Copolymer Surfactants," *Science*, **300**, 460 (2003).

Karlstrom, G., Carlsson, A. and Lindman, B., "Phase Diagrams of Nonionic Polymer/Water Systems: Experimental and Theoretical Studies of the Effects of Surfactants and Other Consolutes," *J. Phys. Chem.*, **94**, 5005 (1990).

Kasas, S., Dumas, G., Dietler, G., Catsicas, S. and Adrian, M., "Vitrification of Cryoelectron Microscopy Specimens Revealed by High-Speed Photographic Imaging," *J. Microsc.-Oxford*, **211**, 48 (2003).

Lambert, O., Letellier, L., Gelbart, W. M. and Rigaud, J. L., "DNA Delivery by Phage as a Strategy for Encapsulating Toroidal Condensates of Arbitrary Size into Liposomes," *PNAS USA*, **97**, 7248 (2000).

Li, X. B., Lin, Z. C., Cai, J., Scriven, L. E. and Davis, H. T., "Polymer-Induced Microstructural Transitions in Surfactant Solutions," *J. Phys. Chem.*, **99**, 10865 (1995).

Lin, Z., "Branched Worm-like Micelles and Their Networks," *Langmuir*, **12**, 1729 (1996).

Mayer, E., "Vitrification of Pure Liquid Water," *J. Microsc.-Oxford*, **140**, 3 (1985).

Pochan, D. J., Pakstis, L., Ozbas, B., Nowak, A. P. and Deming, T. J., "SANS and Cryo-TEM Study of Self-Assembled Diblock Copolypeptide Hydrogels with Rich Nano- through Microscale Morphology," *Macromolecules*, **35**, 5358 (2002).

Porte, G., Gomati, R., Haitamy, O. E., Appell, J. and Marignan, J., "Morphological Transitions of the Primary Surfactant Structures in Brine-Rich Mixtures of Ternary Systems (Surfactant/Alcohol/Brine)," *J. Phys. Chem.*, **90**, 5746 (1986).

Siegel, D. P., Burns, J. L., Chestnut, M. H. and Talmon, Y., "Intermediates in Membrane Fusion and Bilayer Non-bilayer Phase Transitions Imaged by Time-Resolved Cryo-Transmission Electron Microscopy," *Biophys. J.*, **56**, 161 (1989).

Silvander, M., Karlsson, G. and Edwards, K., "Vesicle Solubilization by Alkyl Sulfate Surfactants: A Cryo-TEM Study of the Vesicle to Micelle Transition," *J. Colloid Interface Sci.*, **179**, 104 (1996).

Talmon, Y., "Staining and Drying-Induced Artifacts in Electron Microscopy of Surfactant Dispersions," *J. Colloid Interface Sci.*, **93**, 366 (1983).

Talmon, Y., "Electron Beam Radiation Damage to Organic and Biological Cryospecimens," Cryotechniques in Biological Electron Microscopy, Steinbrecht, R. A. and Zierold, K., eds., Springer-Verlag, Berlin, 64 (1987).

Talmon, Y., "Transmission Electron Microscopy of Complex Fluids: The State of the Art," *Ber. Bunsenges. Phys. Chem.*, **100**, 364 (1996).

Unwin, N., "Acetylcholine-Receptor Channel Imaged in the Open State," *Nature*, **373**, 37 (1995).

Vinson, P. K., "Cryo-Electron and Optical Microscopy of Surfactant Microstructures," PhD, University of Minnesota (1988).

Williams, D. B. and Carter, C. B., "Transmission Electron Microscopy," Plenum Press, New York (1996).

Won, Y.-Y., "Block Copolymer Micelles in Water," Ph.D. Thesis, University of Minnesota, Minneapolis (2000).

Won, Y.-Y., Brannan, A. K., Davis, H. T. and Bates, F. S., "Cryogenic Transmission Electron Microscopy (Cryo-TEM) of Micelles and Vesicles Formed in Water by Poly(ethylene oxide)-Based Block Copolymers," *J. Phys. Chem. B*, **106**, 3354 (2002).

Won, Y.-Y., Davis, H. T. and Bates, F. S., "Giant Wormlike Rubber Micelles," *Science*, **283**, 960 (1999).

Won, Y.-Y., Davis, H. T. and Bates, F. S., "Molecular Exchange in PEO-PB Micelles in Water," *Macromolecules*, **36**, 953 (2003).

Zasadzinski, J. A. N., "A New Heat Transfer Model to Predict Cooling Rates for Rapid Freezing Fixation," *J. Microsc.-Oxford*, **150**, 137 (1988).

Zheng, Y., Lin, Z., Zakin, J. L., Talmon, Y., Davis, H. T. and Scriven, L. E., "Cryo-TEM Imaging the Flow-Induced Transition from Vesicles to Threadlike Micelles," *J. Phys. Chem. B*, **104**, 5263 (2000).

Zheng, Y., Won, Y.-Y., Bates, F. S., Davis, H. T. and Scriven, L. E., "Directly Resolved Core-Corona Structure of Block Copolymer Micelles by Cryo-Transmission Electron Microscopy," *J. Phys. Chem. B*, **103**, 10331 (1999).